Electrostatic Sampler for Collecting Large Regolith Particles on Asteroids

Masato Adachi[1], Takumi Kojima[1], and Hiroyuki Kawamoto[1]
[1]Dept. of Applied Mechanics and Aerospace Engineering
Waseda University
phone: (81) 3-5286-3914
e-mail: masato.a-1019@toki.waseda.jp

***Abstract*—The authors have developed an electrostatic sampler for the reliable and autonomous collection of regolith particles on asteroids. The sampler employs the Coulomb and dielectrophoresis forces to capture the regolith particles and transport them to a collection capsule. In a previous study, it was experimentally verified that the sampler can collect the lunar regolith simulant containing various size particles less than several hundred micrometers in a micro-gravity environment. However, some asteroids would also have large particles with diameters 1.0 mm or larger on their surface. Therefore, in the present study, the authors used numerical calculations and model experiments to confirm whether the sampler can collect particles larger than 1.0 mm in a low-gravity environment. Numerical calculations using the Distinct Element Method predicted the effects of the particle diameter on the sampler performance, indicating that particles 1.0 mm in diameter or larger would be successfully sampled in a low-gravity environment. In addition, glass particles 2 mm in diameter were experimentally sampled in a 0.01-G environment, which was reproduced by the parabolic flight of an aircraft. Moreover, rocks 4 mm in diameter were agitated under 0.01-G, and those would be successfully sampled under micro-gravity.**

I. Introduction

To obtain information about the formative history of asteroids and the solar system, as well as the origin of life, it is necessary to collect samples from asteroids and return them to Earth. The success of the Japan Aerospace Exploration Agency (JAXA) Hayabusa mission, in which samples were retrieved from the asteroid Itokawa, is fresh in our memory [1] [2] [3]. In light of the Hayabusa mission’s success, the JAXA Hayabusa-2 mission has commenced the operation [4]. In addition, some sample return missions have been planned by space agencies worldwide [5] [6]. A durable and reliable sampling system is required for these missions.

Therefore, a unique electrostatic sampler was developed [7] [8]. The sampler causes the Coulomb and dielectrophoresis forces that capture the regolith particles and transport them to a collection capsule. The sampler only utilizes electrostatic force. It does not have mechanical parts, nor require complicated control, thus making it highly reliable. In previous study, it was experimentally verified that the sampler could collect small particles, with diameter less than several hundred micrometers, of the lunar regolith simulant FJS-1 [9]

– which is almost identical to the popular simulant JSC-1A [10] – in a micro-gravity environment reproduced by the parabolic flight of an aircraft [8]. However, some asteroids would keep not only small but also large particles 1.0 mm in diameter or larger. The sampling of large particles is expected to be more difficult than that of small particles because the gravitational force becomes dominant as the particle diameter increases, and it would disturb the moving of large particles. Therefore, an investigation of the possibility of sampling large particles on asteroids is required. In this study, the authors confirmed whether the sampler can collect particles larger than 1.0 mm in a low-gravity environment through numerical calculations and model experiments. The sampler performance at low-gravity was predicted using the three-dimensional Distinct Element Method. Moreover, samplings of 2 mm glass beads and 4 mm rocks were experimentally demonstrated in the low-gravity environment created by the parabolic flight of an aircraft.

II. System Configuration

Fig. 1 and Fig. 2 show the design of the electrostatic sampler and the experimental procedure, respectively. When a rectangular two-phase high voltage (10 kV_{p-p}) is applied between the parallel screen electrodes (wire diameter: 1.3 mm, pitch: 10 mm, gap: 10 mm), which are attached to the lower end of a sampling tube (inner diameter: 50 mm) and the lower screen electrode touches the particles, the resultant Coulomb and dielectrophoresis forces act on the particles near the electrodes. If these forces exceed the gravitational force and the force of adhesion to the asteroid, the particles are agitated and float. Some of these particles pass through the openings of the screen electrodes (Fig. 2 (a)) and are transported to a collection capsule located in the upper 120 mm of the upper electrodes because of their own inertia force. After the operation for 5.0 s, a stopper plate closes the collection capsule to retain the particles (Fig. 2 (b)). Details about the sampling mechanism are presented in the literature [8].

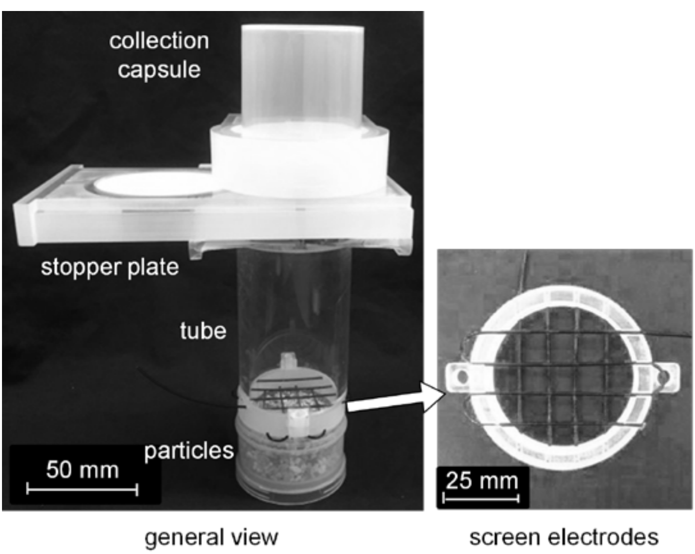

Fig. 1. Design of electrostatic sampler

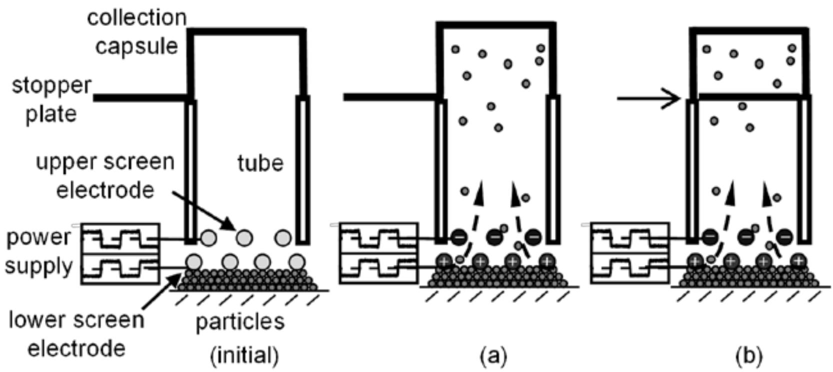

Fig. 2. Experimental procedure

Glass beads and rocks were used for the experiment as shown in Fig. 3 (a) and (b). Fig. 3 shows the size distribution of the particles. The most of glass beads were around 2 mm in diameter. The glass beads were largely made of silicon dioxide, which is the main component in lunar regolith [11]. On the other hand, the most of the rocks are around 4 mm in diameter, and their compositions are similar to that of the lunar regolith simulant. These particles were initially set in the container (height: 0.3 mm, inner diameter: 50 mm), and their behaviors during the sampler operation were observed using a high-speed camera (GZ-V590, JVC KENWOOD, Kanagawa, JAPAN).

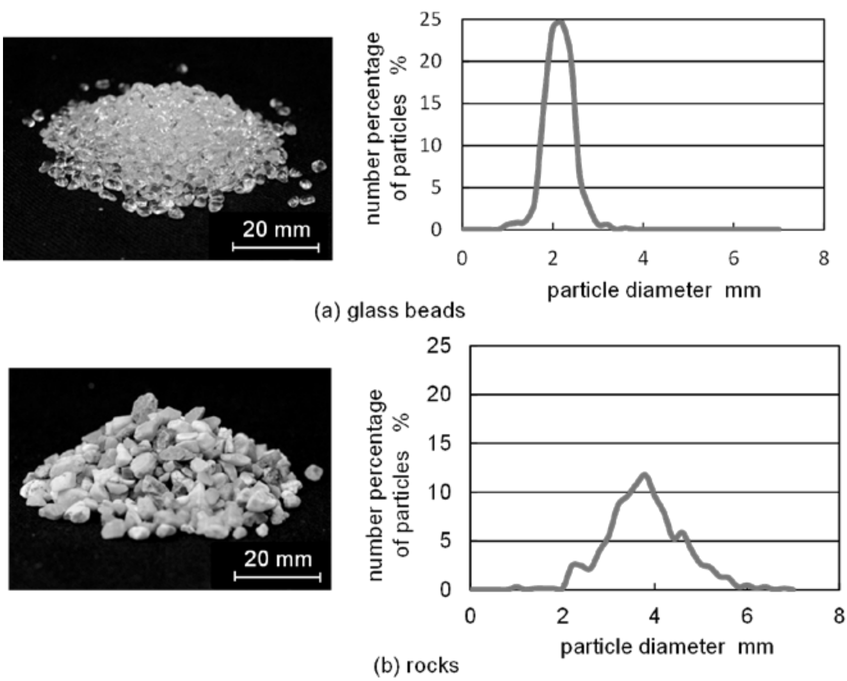

Fig. 3. (a) Glass beads and (b) rocks and their size distribution

III. Numerical Calculation

Both numerical calculations and model experiments are performed to predict and investigate the particle dynamics under the sampler operation. Numerical calculations were performed using a hard sphere model of the three-dimensional Distinct Element Method. The equations of motion for the *i*-th particle are given by Equations (1):

$$m_i \ddot{\boldsymbol{x}}_i = -6\pi\eta R \dot{\boldsymbol{x}}_i + \boldsymbol{F}_q + \boldsymbol{F}_{dielectro} + \boldsymbol{F}_g + \boldsymbol{F}_{adhesion} \tag{1}$$

where $\boldsymbol{x}$: the displacement vector, = (x, y, z), η: the viscosity of air (=1.8×10^{-5} [Pa·s] at 1 atm), m: the particle mass, R: the particle radius. Equation (1) indicates that the particle motion is affected by the air drag as well as Coulomb, dielectrophoresis, gravitational, and adhesion forces, which are represented by Equations (2), (3), (4), and (5), respectively [12]:

$$\boldsymbol{F}_q = q_i \boldsymbol{E} \tag{2}$$

$$\boldsymbol{F}_{dipole} = 2\pi\varepsilon_0 \frac{\varepsilon_r - \varepsilon_0}{\varepsilon_r + 2\varepsilon_0} R_i^{\,3} \nabla E^2 \tag{3}$$

$$\boldsymbol{F}_g = m_i \boldsymbol{g} \tag{4}$$

$$\boldsymbol{F}_{adhesion} = -\alpha \left(\frac{R_i R_k}{R_i + R_k} \right) \boldsymbol{n} \tag{5}$$

where q: the particle charge, $\boldsymbol{E}$: the electrostatic field, ε_r: the relative permittivity (1.0 for air, 2.5 for particle), ε_0: the permittivity of free space (8.8×10^{-12} [F/m]), $\boldsymbol{g}$: gravitational acceleration, α: the correction coefficient of adhesion force (0.00027), and $\boldsymbol{n}$: the unit normal vector from the k-th object to the i-th particle. The charge of the particles, which ranged from less than 100 μm to 1.2 mm in diameter, was measured using the free-fall method [13] and reported in the literature [8]. Fig. 4 shows the measured charge distribution. The authors assumed that the charge ratio decreases with the particle size, and two approximate equations for the positively and negatively charge ratios were estimated. The charge of the particles was randomly determined as equal to or smaller than the absolute value of the assumed equations as shown in Fig. 4. The external electrostatic field $\boldsymbol{E}$ generated by the sampler was calculated using the three-dimensional finite differential method. The particle was assumed to be the lunar regolith simulant FJS-1, and its mass was estimated according to the specific gravity of FJS-1 (= 2700 [kg/m^3]). The coefficient of the adhesion force α was obtained from the literature [8]. Under a vacuum environment, the air drag can be neglected. The torque on the particle was assumed to be zero. The scale of the experimental set-up, including the sampling tube and parallel screen electrodes, was reproduced in the numerical calculations. All of the particles were randomly placed beneath the lower screen electrode. Equation (1) was solved using the Runge-Kutta method at each time step. The velocities after particle-particle and particle-object collisions were calculated using the modified hard sphere model, which is described in detail in the literature [12]. Particles that reached a height of 120 mm within 5.0 s of the sampler operation were deemed to be collected.

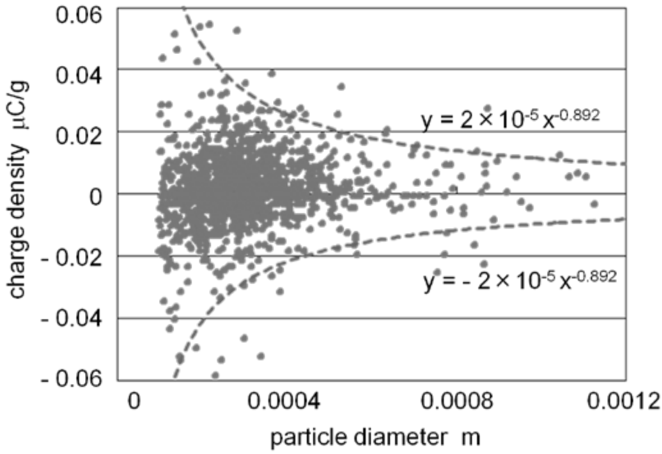

Fig. 4. Charge distribution of particles as measured by free-fall method

IV. Results and Discussion

Fig. 5 and Fig. 6 show the calculated amount of collected particles for each diameter with respect to the frequency of the applied voltage in air and a vacuum, respectively. Fig. 7 shows the calculated particle behavior; here, the colors indicate the dominant external force. These calculations are performed under the application of 10 $kV_{p\text{-}p}$ voltage at 0.00001-G. Fig. 5 shows that the optimum frequency, approximately 1–3 Hz for the applied voltage, exists for all particles. This is because the infrequent polarity change of the applied voltage during the short duration of 5.0 s reduces the sampler performance. On the other hand, the high-frequently change of the polarity prevents particles that are in vertically vibrational motion between the parallel screen electrodes from passing through the opening of the upper electrode. These tendencies agree with the results for particles smaller than 1 mm, as described in the literature [8].

The amount of collected particles decreases as the particle diameter increases. This is because relatively large dielectrophoresis force acts on large particles. Air drag is not the reason why the sampling of large particles is difficult because the amount of collected particles hardly changes between air and vacuum, as shown in Fig. 5 and Fig. 6. Moreover, the extremely small gravitational force can be neglected. As shown in Fig. 7, the particles between parallel electrodes are largely affected by the dielectrophoresis force. This dielectrophoresis force acts as an attractive force to the electrodes, as the electrostatic field strength increases with proximity to the electrodes. Therefore, the dielectrophoresis force tears particles off the asteroid (Fig. 7 (a), 0.0 s) and attracts them to the space between the parallel electrodes (Fig. 7 (a), 0.25 s). Subsequently, although some particles are transported above the upper screen electrode by the Coulomb force, the dielectrophoresis force keeps most of the particles between the parallel screen electrodes (Fig. 7 (a), 2.5 s). For the successful sampling, it is necessary to apply the dielectrophoresis force optimally. For example, if one pulsing voltage is applied to the electrodes, the resultant pulsing dielectrophoresis force is utilized only to tear particles off the asteroid; then, particles are transported upward by their own inertia force.

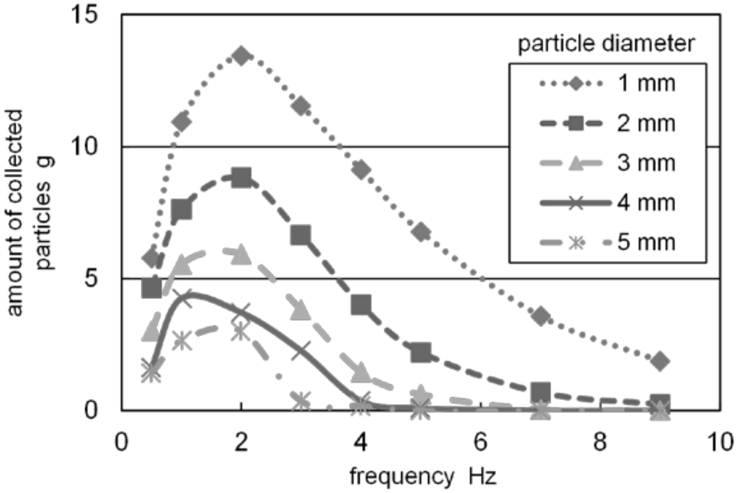

Fig. 5. Calculated amount of collected particles under application of 10 kV_{p-p} in air at 0.00001-G

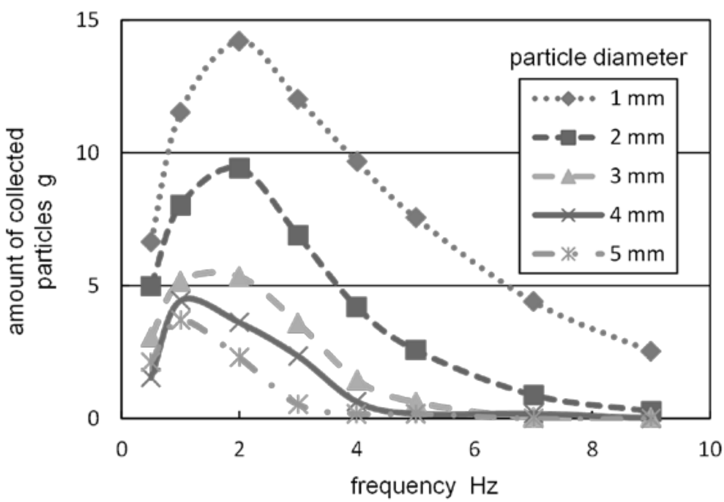

Fig. 6. Calculated amount of collected particles under application of 10 kV_{p-p} in vacuum at 0.00001-G

The second reason why the sampling of large particles is difficult is that large particles easily jam the screen electrodes. Fig. 7 (b) shows that small particles 1 mm in diameter smoothly pass through the screen electrodes, and that numerous particles are transported above. On the other hand, the 5 mm particles collide with the upper electrodes (Fig. 7 (a), 0.5 s). Moreover, the particles between the parallel electrodes obstruct other particles from passing through the upper electrode (Fig. 7 (a), 2.5 s). To sample large particles, the pitch of the screen electrodes should be larger than the size of the objective particle.

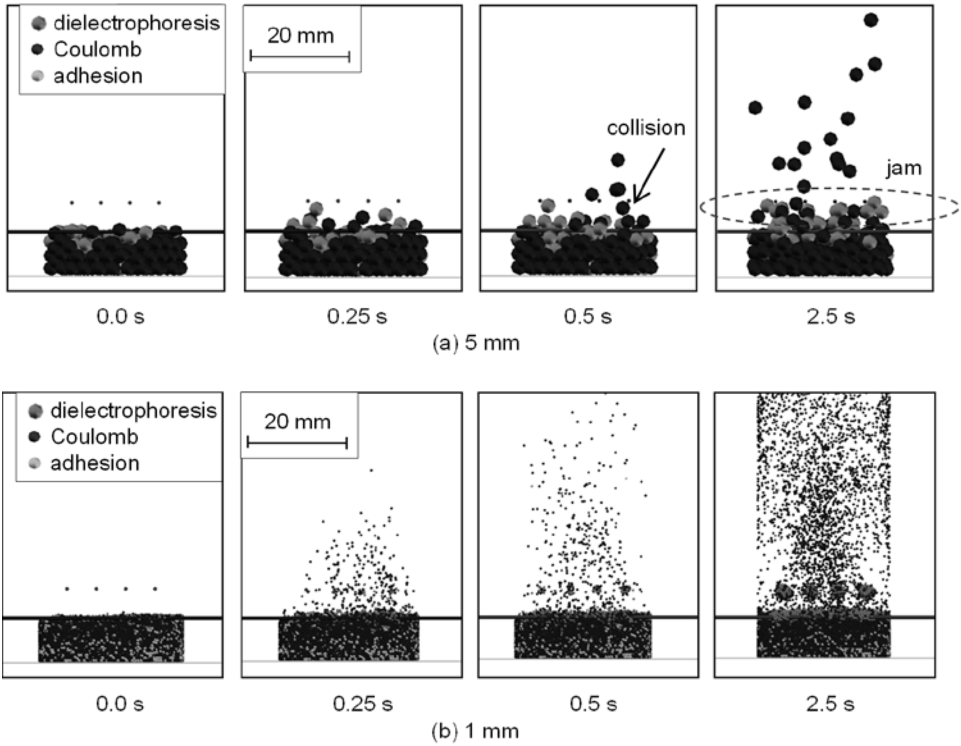

Fig. 7. Calculated behaviors of particles, (a) 5 mm and (b) 1 mm in diameter, under application of 10 kV_{p-p} in vacuum at and 0.00001-G

Fig. 8 shows the calculated amount of collected particles for each diameter with respect to the gravitational acceleration. As indicated by Fig. 8, the successful sampling depends on the gravitational acceleration. Although the amounts of collected particles are saturated at a gravitational acceleration below 0.0001-G for 1- 4 mm particles, they decrease as the gravitational acceleration increases beyond 0.0001-G because the gravitational force prevents particles from moving. Particles 1-5 mm in diameter could not be collected at a gravitational acceleration of 0.1-G or higher. The amounts of collected 5 mm particles increase as the gravitational acceleration decreases below 0.0001-G, and those would be saturated under the gravitational acceleration less than 0.000001-G. The calculated results indicate that the sampling of particles is easier at a low gravitational acceleration. We expected the successful sampling of particles ranging in diameter from less than 1 mm to 5 mm in a low-gravity environment at less than 0.001-G.

To compare the aforementioned calculated results and confirm the performance of the sampler, sampling experiments were conducted. In light of the calculated results, the sampling particles at 1-G would be impossible; therefore, the experiments were performed under a low-gravity environment, which was reproduced by the parabolic flight of an aircraft, for approximately 5.0 s.

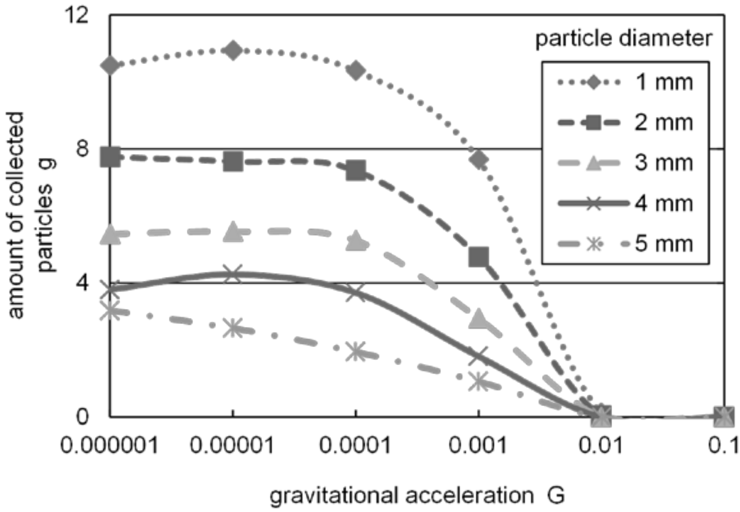

Fig. 8. Calculated amount of collected particles under the application of 10 $kV_{p\text{-}p}$ at 1 Hz in air

Table. 1 shows the average gravitational acceleration in each experimental condition. The parabolic flight was operated to keep the gravitational acceleration from being lower than 0-G, and it was kept around the 0.01-G. For the frequency of 3 Hz, the average of the gravitational acceleration was larger than others.

Table.1 Average gravitational acceleration during parabolic flight

1 Hz	3 Hz	5 Hz	7 Hz	9 Hz
0.0112-G	0.0229-G	0.0174-G	0.0135-G	0.0164-G

Fig. 9 (a) shows the observed glass beads behaviors and Fig. 9 (b) shows the calculated results for the 2 mm particles. These were conducted under the application of 10 $kV_{p\text{-}p}$ at a 1.0 Hz voltage in air at 0.01-G. The particles’ motions were observed from an angle that differed from that used in the calculation. Glass beads near the lower electrodes were agitated, and some passed through the openings of the electrodes (Fig. 9 (a) 0.25 s). Some particles reached the collection capsule, as predicted by the numerical calculations (Fig. 9 (b)). In addition, the results of the experiment and calculations indicate that some particles adhered to the surface of the electrode (Fig. 9 (a), (b) 1.0 s). This is because a large dielectrophoresis force attracts particles to the electrode. Fig. 10 (a) shows the calculated and measured amounts of collected particles. Under the application of 5 Hz, 0.18 g of glass beads were successfully sampled as shown in Fig. 10 (b). The measured value quantitatively agreed with the calculated results. At 3 Hz, the amount of collected particles was small because the average gravitational acceleration was larger than in other conditions, as shown in Table. 1, thus making it low performance.

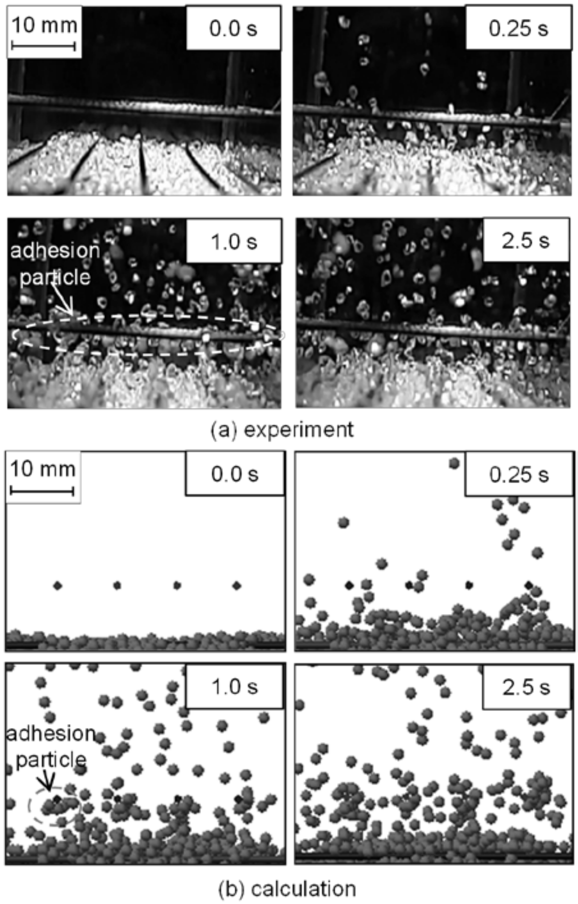

Fig. 9. (a) Observed glass beads and (b) calculated particles 2 mm in diameter under application of 10 kV_{p-p} at 1 Hz in air at 0.01-G

Fig. 11 shows the observed motions of the rocks and the calculated motions of 4 mm particles under the application of 10 kV_{p-p} at 1.0 Hz in air at 0.01-G. The rocks were agitated, and some passed through the openings of the electrodes (Fig. 11, (a) 0.25 s); however, they could not reach the collection capsule and fell down immediately because of the relatively large gravitational force acting on large particles (Fig. 11 (a), 1.0 s). These results agreed with the prediction by the numerical calculations (Fig. 11 (b)). As predicted, particles larger than 3 mm would be sampled under a low-gravity environment below 0.001-G, as shown in Fig. 8.

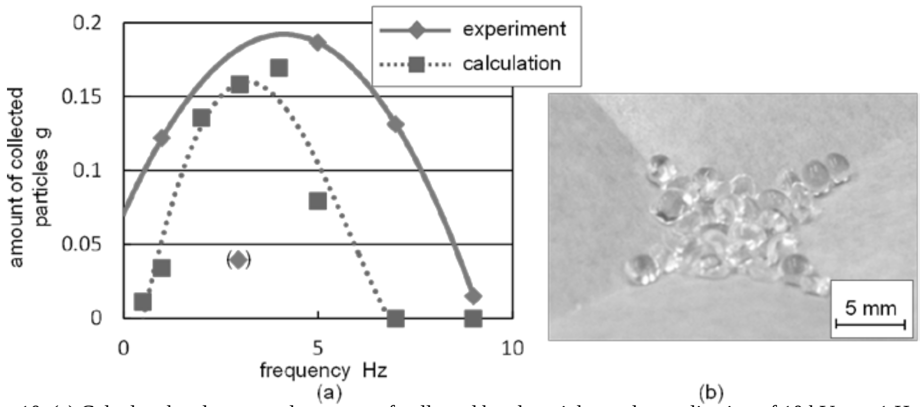

Fig. 10. (a) Calculated and measured amounts of collected bead particles under application of 10 kV_{p-p} at 1 Hz in air at 0.01-G, and (b) collected glass beads with mass of 0.18 g

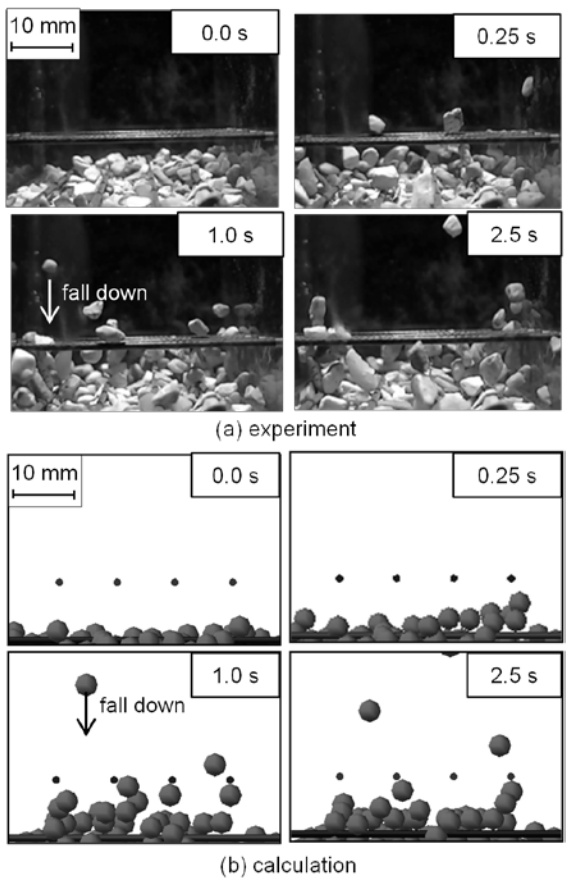

Fig. 11. (a) Observed motion of rocks and (b) calculated result of 4 mm particles under the application of 10 kV_{p-p} at 1 Hz in air at 0.01-G

V. Conclusion

The authors have developed a unique sampler that reliably samples large particles on an asteroid surface. The performance of the electrostatic sampler for particles larger than 1 mm in a low-gravity environment was confirmed by numerical calculations and model experiments. According to the results, 2 mm glass beads are successfully sampled at a gravitational acceleration of 0.01-G, and 4 mm rocks would be successfully sampled below 0.001-G.

Acknowledgement

The authors express their gratitude to Yuki Maezono and Tomoki Sakata (Waseda Univ.) for their support in conducting the experiment.

References

[1] H. Kuninaka, and J. Kawaguchi, "Lessons Learned from round Trip of HAYABUSA Asteroid Explorer in Deep Space." *Aerospace Conference 2011 IEEE*, pp.1-8, 2011.

[2] T. Noguchi, T. Nakamura, M. Kimura, M. E. Zolensky, M. Tanaka, T. Hashimoto, M. Konno, A. Nakato, T. Ogami, A. Fujimura, M. Abe, T. Yada, T. Mukai, M. Ueno, T. Okada, K. Shirai, Y. Ishibashi, and R. Okazaki, "Incipient Space Weathering Observed on the Surface of Itokawa Dust Particles." *Science*, 333 (6046), pp.1121-1125, 2011.

[3] A. Tsuchiyama, M. Uesugi, T. Matsushima, T. Michikami, T. Kadono, T. Nakamura, K. Uesugi, T. Nakano, S. A. Sandford, R. Noguchi, T. Matsumoto, J. Matsuno, T. Nagano, Y. Imai, A. Takeuchi, Y. Suzuki, T. Ogami, J. Katagiri, M. Ebihara, T. R. Ireland, F. Kitajima, K. Nagao, H. Naraoka, T. Noguchi, R. Okazaki, H. Yurimoto, M. E. Zolensky, T. Mukai, M. Abe, T. Yada, A. Fujimura, M. Yoshikawa, and J. Kawaguchi, "Three-dimensional structure of Hayabusa samples: origin and evolution of Itokawa regolith." *Science*, 333 (6046), 1125-1128, 2011.

[4] Y. Tsuda, M. Yoshikawa, M. Abe, H. Minamino, and S. Nakazawa, "System design of the hayabusa 2—asteroid sample return mission to 1999 JU3." *Acta Astronautica*, 91, 356-362, 2013.

[5] D. S. Lauretta, and The OSIRIS-REx Team, "An overview of the OSIRIS-REx asteroid sample return mission." *43rd Lunar and Planetary Science Conference*, 19-23, 2012.

[6] P. Michel, M. A. Barucci, A. F. Cheng, H. Bohnhardt, J. R. Brucato, E. Dotto, P. Ehrenfreund, I. A. Franchi, S. F. Green, L. M. Lara, B. j. Marty, D. Koschny, and D. Agnolon, "Marcopolo-r: Near-earth asteroid sample return mission selected for the assessment study phase of the ESA program cosmic vision." *Acta Astronautica*, 93, 530-538, 2014.

[7] H. Kawamoto, "Sampling of Small Regolith Particles from Asteroids Utilizing Alternative Electrostatic Field and Electrostatic Traveling Wave." *J. Aerospace Engineering*, 27(3), 631-635, 2014.

[8] M. Adachi, H. Maezono, and H. Kawamoto, "Sampling of Regolith on Asteroids Using Electrostatic Force", *J. Aerospace Engineering*, 27(3), 631-635, 2014 (submitted).

[9] H. Kanamori, S. Udagawa, T. Yoshida, S. Matsumoto, and K. Takagi, "Properties of lunar soil stimulant manufactured in Japan." *Proc., 6th Int. Conf. on Engineering, Construction and Operations in Space*, ASCE, Reston, VA, 462–468, 1998.

[10] C. C. Allen, R. V. Morris, D. J. Lindstrom, M. M. Lindstrom, and J. P. Lockwood, "JSC Mars-1: Martin Regolith Simulant." *Lunar and Planetary Science XXVIII*, Abstract#1797, 1997.

[11] D. S. McKay, et al., "The lunar regolith." Lunar sourcebook, Heiken, G., Vaniman, D., and French, B. M. eds., Cambridge University Press, Cambridge, UK, 285-356, 1991.

[12] M. Adachi, and H. Kawamoto, "Electrostatic dust shield system used for Lunar and Mars exploration equipment", *Transactions of the JSME*, 81, 821, 2014. (in Japanese).

[13] H. Kawamoto, K. Seki, and N. Kuromiya, "Mechanism of travelling-wave transport of particles." *J. Physics D: Applied Physics*, 39 (6), 1249-1256, 2006.